NUCLEAR DATA AND MEASUREMENTS SERIES

ANL/NDM-113

Resonance Effects in Neutron Scattering Lengths

by

J.E. Lynn

June 1989

**ARGONNE NATIONAL LABORATORY,
ARGONNE, ILLINOIS 60439, U.S.A.**

NUCLEAR DATA AND MEASUREMENTS SERIES

ANL/NDM-113

RESONANCE EFFECTS
IN NEUTRON SCATTERING LENGTHS

by

J. E. Lynn

June 1989

ARGONNE NATIONAL LABORATORY, ARGONNE, ILLINOIS

Argonne National Laboratory, with facilities in the states of Illinois and Idaho, is owned by the United States government, and operated by The University of Chicago under the provisions of a contract with the Department of Energy.

ANL/NDM-113

RESONANCE EFFECTS

IN NEUTRON SCATTERING LENGTHS*

by

J. E. Lynn†

June 1989

NEUTRON SCATTERING LENGTHS. Neutron scattering
lengths and nuclear effects giving rise to their variation
are discussed.

Engineering Physics Division
ARGONNE NATIONAL LABORATORY
9700 South Cass Avenue
Argonne, Illinois 60439
U.S.A.

NUCLEAR DATA AND MEASUREMENTS SERIES

The Nuclear Data and Measurements Series presents results of studies in the field of microscopic nuclear data. The primary objective is the dissemination of information in the comprehensive form required for nuclear technology applications. This Series is devoted to: a) measured microscopic nuclear parameters, b) experimental techniques and facilities employed in measurements, c) the analysis, correlation and interpretation of nuclear data, and d) the evaluation of nuclear data. Contributions to this Series are reviewed to assure technical competence and, unless otherwise stated, the contents can be formally referenced. This Series does not supplant formal journal publication, but it does provide the more extensive information required for technological applications (e.g., tabulated numerical data) in a timely manner.

TABLE OF CONTENTS

INFORMATION ABOUT OTHER ISSUES OF THE ANL/NDM SERIES

A list of titles and authors for all the previous issues appears in each report of the series. The list for reports ANL/NDM–1 through ANL/NDM–75 appears in ANL/NDM–76, and ANL/NDM–91 contains the list for reports ANL/NDM–76 through ANL/NDM–90. Below is the list for ANL/NDM–91 up to the current report. Requests for a complete list of titles or for copies of previous reports should be directed to:

Section Secretary
Applied Nuclear Physics Section
Engineering Physics Division
Building 316
Argonne National Laboratory
9700 South Cass Avenue
Argonne, Illinois 60439
U.S.A.

ANL/NDM–91 A.B. Smith, P.T. Guenther and R.D. Lawson, *On the Energy Dependence of the Optical Model of Neutron Scattering from Niobium*, May 1985.

ANL/NDM–92 Donald L. Smith, *Nuclear Data Uncertainties (Vol.–I): Basic Concepts of Probability*, December 1988.

ANL/NDM–93 D.L. Smith, J.W. Meadows and M.M. Bretscher, *Integral Cross–section Measurements for $^{7}Li(n,n't)^{4}He$, $^{27}Al(n,p)^{27}Mg$, $^{27}Al(n,\alpha)^{24}Na$, $^{58}Ni(n,p)^{58}Co$, and $^{60}Ni(n,p)^{60}Co$ Relative to ^{238}U Neutron Fission in the Thick–target $^{9}Be(d,n)^{10}B$ Spectrum at $E_d = 7\,MeV$*, October 1985.

ANL/NDM–94 A.B. Smith, D.L. Smith, P. Rousset, R.D. Lawson and R.J. Howerton, *Evaluated Neutronic Data File for Yttrium*, January 1986.

ANL/NDM–95 Donald L. Smith and James W. Meadows, *A Facility for High–intensity Neutron Irradiations Using Thick–target Sources at the Argonne Fast–neutron Generator*, May 1986.

ANL/NDM–96 M. Sugimoto, A.B. Smith and P.T. Guenther, *Ratio of the Prompt–fission–neutron Spectrum of Plutonium–239 to that of Uranium–235*, September 1986.

ANL/NDM–97 J.W. Meadows, *The Fission Cross Sections of ^{230}Th, ^{232}Th, ^{233}U, ^{234}U, ^{236}U, ^{238}U, ^{237}Np, ^{239}Pu, and ^{242}Pu Relative ^{235}U at 14.74 MeV Neutron Energy*, December 1986.

ANL/NDM–98 J.W. Meadows, *The Fission Cross Section Ratios and Error Analysis for Ten Thorium, Uranium, Neptunium and Plutonium Isotopes at 14.74–MeV Neutron Energy*, March 1987.

ANL/NDM–99 Donald L. Smith, *Some Comments on the Effects of Long–range Correlations in Covariance Matrices for Nuclear Data*, March 1987.

ANL/NDM–100 A.B. Smith, P.T. Guenther and R.D. Lawson, *The Energy Dependence of the Optical–model Potential for Fast–neutron Scattering from Bismuth*, May 1987.

ANL/NDM–101 A.B. Smith, P.T. Guenther, J.F. Whalen and R.D. Lawson, *Cobalt: Fast Neutrons and Physical Models*, July 1987.

ANL/NDM–102 D. L Smith, *Investigation of the Influence of the Neutron Spectrum in Determinations of Integral Neutron Cross–Section Ratios*, November 1987.

ANL/NDM–103 A.B. Smith, P.T. Guenther and B. Micklich, *Spectrum of Neutrons Emitted From a Thick Beryllium Target Bombarded With 7 MeV Deuterons*, January 1988.

ANL/NDM–104 L.P. Geraldo and D.L. Smith, *Some Thoughts on Positive Definiteness in the Consideration of Nuclear Data Covariance Matrices*, January 1988.

ANL/NDM–105 A.B. Smith, D.L. Smith, P.T. Guenther, J.W. Meadows, R.D. Lawson, R.J. Howerton, and T. Djemil, *Neutronic Evaluated Nuclear–Data File for Vanadium*, May 1988.

ANL/NDM–106 A.B. Smith, P.T. Guenther, and R.D. Lawson, *Fast–Neutron Elastic Scattering from Elemental Vanadium*, March 1988.

ANL/NDM–107 P. Guenther, R. Lawson, J. Meadows, M. Sugimoto, A. Smith, D. Smith, and R. Howerton, *An Evaluated Neutronic Data File for Elemental Cobalt*, August 1988.

ANL/NDM–108 M. Sugimoto, P.T. Guenther, J.E. Lynn, A.B. Smith, and J.F. Whalen, *Some Comments on the Interaction of Fast–Neutrons with Beryllium*, November 1988.

ANL/NDM–109 P.T. Guenther, R.D. Lawson, J.W. Meadows, A.B. Smith, D.L. Smith, and M. Sugimoto, *An Evaluated Neutronic Data File for Bismuth*, March 1989 (not yet printed)

ANL/NDM–110 D.L. Smith and L.P. Geraldo, *A Vector Model for Error Propatation*, March 1989.

ANL/NDM–111 J.E. Lynn, *Fifty Years of Nuclear Fission*, June 1989.

ANL/NDM–112 S. Chiba, P.T. Guenther, and A.B. Smith, *Some Remarks on the Neutron Elastic– and Inelastic–Scattering Cross Sections of Palladium*, May 1989.

RESONANCE EFFECTS

IN NEUTRON SCATTERING LENGTHS*

by

J. E. Lynn†

Abstract

The nature of neutron scattering lengths is described and the nuclear effects giving rise to their variation is discussed. Some examples of the shortcomings of the available nuclear data base, particularly for heavy nuclei, are given. Methods are presented for improving this data base, in particular for obtaining the energy variation of the complex coherent scattering length from long to sub—Angstrom wave lengths from the available sources of slow neutron cross section data. Examples of this information are given for several of the rare earth nuclides. Some examples of the effect of resonances in neutron reflection and diffraction are discussed. This report documents a seminar given at Argonne National Laboratory in March 1989.

---

†Argonne Fellow. Permanent address: UKAEA, Harwell, Oxon OX11 ORA, United Kingdom.

RESONANCE EFFECTS IN NEUTRON SCATTERING LENGTHS

J.E.Lynn*

Argonne National Laboratory
Argonne, Illinois 60439

1. Introduction

To a nuclear physicist surveying the opportunities now being opened up in the field of neutron scattering techniques for condensed matter research, particularly by the intense spallation neutron sources that can operate well into the sub-Ångström region, it is clear that the readily accessible nuclear data base for this work is far from satisfactory. It is my purpose in this seminar to describe the current situation in the data base as I see it, and in particular to discuss the neutron coherent scattering lengths of the heavy nuclides, which often have strong energy dependences and imaginary components owing to nuclear resonances in their cross-sections.

The solid-state physicist primarily wishes to regard the nuclei off which his neutrons scatter as tiny impenetrable spheres, the Fermi pseudo-potentials, which are only characterized by their effective "radius", the scattering length. The fact that they are much more than that is already apparent from surveying the neutron scattering properties of the very lightest nuclides. First of all, we have the strong isotope variation; examples are

$$^1\text{H} \qquad a_{coh} = -1.87 \text{ fm} \quad (-0.187 \ 10^{-12} \text{ cm})$$

$$^2\text{H} \qquad a_{coh} = 4.45 \text{ fm}$$

(a denotes free atom scattering length). The fact that the proton scattering length is negative also shows the inadequacy of the particle picture. Then there is the spin difference. Defining the channel spin s as the resultant of the nucleus and neutron spins, we have the examples;

$$^1\text{H} \qquad a_{s=1} = 5.42 \text{ fm}$$

$$a_{s=0} = -23.75 \text{ fm}$$

$$^2\text{H} \qquad a_{s=3/2} = 6.34 \text{ fm}$$

$$a_{s=1/2} = 0.65 \text{ fm}$$

Thirdly, we have the possibility of sizeable imaginary components. The lightest nuclide in this class is ^3He, with a bound atom coherent scattering length of

$$b_{coh} = 5.73 - i1.48 \text{ fm}$$

---

*Argonne Fellow: permanent address; UKAEA, Harwell, Oxon OX11 0RA, England

All these features are consequences of nuclear excitation levels. Because the neutron energy range of interest to the condensed matter scientist is so tiny compared to the energy scale of the nuclear levels in these examples, there is no energy variation of any significance, but the isotope and spin variations are of major use.

The data base seems to be quite sound for many of the light nuclides. For heavier nuclides, however, there appear to be many gaps and anomalies, even before we begin to consider the consequences of the much more closely spaced nuclear levels in these systems. As an example of the cause for concern about the available data base, I show a table of the data for samarium and its isotopes as it could well appear in the kind of compilation easily available to the neutron scatterer at the present time (this Table is only slightly disguised from an actual one).

Table 1. *State of the Nuclear Data Base for heavy nuclides*

Typical case: Samarium and its isotopes

Isotope	a (fm)	λ (Å)	Comment
natSm	0.7±0.2	1.86	From measurement[1]
	0.0±0.05	1.30	From measurement[2]
	-0.12±0.04	1.27	From measurement[3]
	4.2±0.3		From compilation[4]
	1.4	1.80	From compilation[4]
	2.9±0.06	1.30	Meas.[2] (Imag.comp.)
	-1.5	1.80	Comp.[4] (Imag.comp.)
144Sm	4.4±4.0		From compilation[5]
147Sm	14.0±3.0		From compilation[4]
148Sm	33.0±6.0		From compilation[5]
149Sm	-24.0-i11.0	1.80	From compilation[4]
	-18.7±0.28	1.80	From measurement[6]
150Sm	14.0±3.0		From compilation[4]
152Sm	-5.0±0.6		From measuremant[7]
154Sm	9.25±1.0		From compilation[4]
	8.0±1.0		From measurement[7]

We see from this Table that, firstly, the entries in commonly used compilations do not necessarily agree, even qualitatively, with measured and well-documented values. Secondly, there are a number of nuclides for which directly measured scattering lengths do not exist, yet values are given in compilations; in the compilations referred to above, no argument or evidence is advanced for the

numbers quoted. There appear to be almost 60 elements and isotopes for which only this kind of value is available.

Thirdly, there is a sign discrepancy for the imaginary components of the scattering length of the natural element. There has been a degree of arbitrariness in the literature over the choice of sign for the imaginary part; subsequently in this report, I employ the negative sign that comes naturally from the deduction of the scattering length from nuclear reaction theory (see also Sears' on this point).

Finally, there is a wave-length variation in the scattering for natural samarium, which is due to a strong resonance in ^{149}Sm at low energy. In compilations, this wave-length variation is seldom made very obvious, even though in a few cases, such as natural samarium and its resonant isotope, a series of measurements from long wavelength to just below 1Å have been made[3,6]. It is my main purpose in this report to show how existing cross-section data can be used to give better scattering length data, including especially the systematic energy variation and phase component that are important for very many heavy nuclides.

2. Theory of neutron scattering lengths

The expansion in spherical polar coordinates of a plane wave travelling in the z direction with velocity v is, ignoring neutron and target spin effects,

$$\exp(ikz) = \frac{\sqrt{\pi}}{kr\sqrt{v}} \sum_{\ell=0}^{\infty} i^{\ell+1} [I_\ell(kr) - O_\ell(kr)] Y_{\ell 0}(\theta,\varphi) \qquad (1)$$

Here, k is the neutron wave number, $Y_{\ell 0}(\theta,\varphi)$ are spherical harmonics and I, O are combinations of spherical bessel and neumann functions and have the form of incoming and outgoing waves. Ignoring the centre-of-mass factor for the heavy nuclei considered in this report k has the numerical value

$$k = 0.0021968 \sqrt{E}$$

in units of 10^{12} cm^{-1}, where E is the neutron energy in electron-volts (eV).

For $\ell = 0$, $I_0 = \exp(-ikr)$, $O_0 = \exp(ikr)$, so we can write

$$\exp(ikz) = (\sqrt{\pi}/kr\sqrt{v})[2\sin(kr)/\sqrt{4\pi} + \Sigma_{\ell \geq 1} i^{\ell+1}(I_\ell - O_\ell)Y_{\ell 0}(\theta,\varphi)] \qquad (2)$$

For $kr \ll 1$, $\ell \geq 1$, $I - O$ is negligible, so the effect of a nuclear potential confined to a region with radius R satisfying the first condition on these waves of higher angular momentum is unimportant for the scattering of the plane wave.

For a hard sphere of radius R, the wave-function has a node at R and is zero within the sphere. Hence the form of the wave-function of the impinging projectile plus scattering is

$$\Psi \propto \sin[k(r-R)]/kr \qquad (3)$$

This can be written in the form of incoming and outgoing waves as

$$\Psi \propto \exp(ikR)[\exp(-ikr) - \exp(-2ikR)\exp(ikr)] \qquad (4)$$

The amplitude of the scattered wave [$\propto (\sin k(r-R) - \sin kr)$] is approximately proportional to R, showing that this is the scattering length for a hard sphere. More accurately, the proportionality of the scattered wave amplitude can be written as [$1 - \exp(-2ikR)$].

The physical situation described above is that in which the only channel is the elastic one. Here I define the concept of a channel. A channel is the distinct separation of a reacting nuclear system into two entities, one a residual (or target) nucleus, the other an ejectile (or projectile), each in a particular state of excitation and spin. Neutron cross-sections can be expressed in terms of a collision matrix **U**, which is the set of amplitudes of the outgoing wave-functions produced in the exit channels as a result of a neutron reaction with a target nucleus. For many purposes the most significant of these amplitudes is that for elastic scattering, from which can be deduced the elastic scattering cross-section, the total cross-section and the absorption cross-section (the sum of all cross-sections into non-elastic channels), and I shall limit our discussion henceforth to this one amplitude, which I shall denote by U.

In a plane wave the amplitude of the outgoing wave-function in the elastic channel relative to that of the incoming wave is unity. The form of the scattering wave-function is therefore proportional to $(1-U)$. In the example above U is just $\exp(-2ikR)$. For a potential well, rather than a rigid sphere, the quantity R is replaced by an apparent "radius" R', which has the form illustrated in Fig.1; this is actually the phase shift (divided by k) for the elastic scattering. This quantity can be visualised as the linear extrapolation of the sine wave outside the well to its node. This is illustrated in Fig.2 in which a resonance condition is achieved when the wave function inside the well contains exactly an odd number of quarter wavelengths and an infinite scattering length ensues. At an energy slightly below resonance the extrapolated value of the node (scattering length) is small, or even negative, while above resonance it is positive and much larger than the well radius. As a function of projectile energy the apparent radius for a specific potential well will have the form shown in Fig.3.

Translated into nuclear physics, in which the nuclear radius is approximately proportional to the cube root of the nuclear mass number A, the phase shift has the mass number dependence shown in Fig.4, the strong swings occurring as the potential well radius passes through the resonance condition for very low neutron energy, and it is found that nuclear scattering lengths do have a very rough and ready mass number dependence of this kind. Again translated to nuclei, the resonance effects apparent in Fig.3 would have spacing on a scale of several MeV.
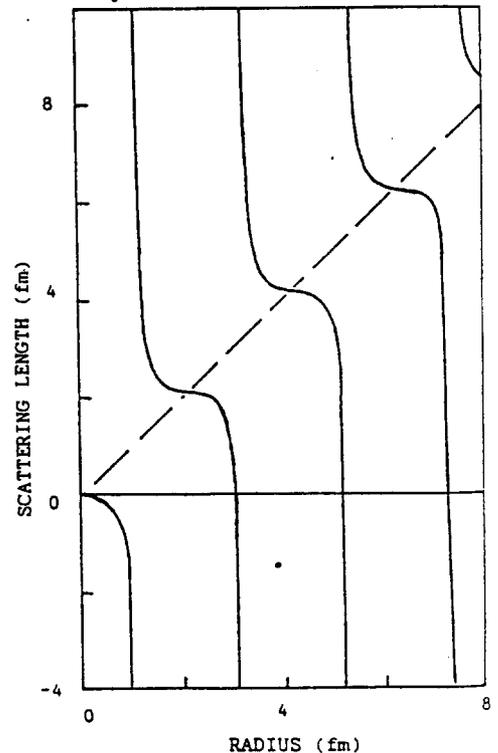

Figure 1. Scattering length as function of radius of a potential well. The broken line is for an impenetrable sphere.
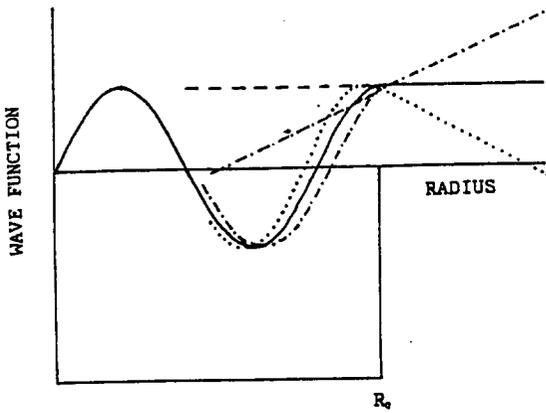
Figure 2.Wave function at resonance (full curve), below resonance (dot-dash) and above resonance (dotted). The node of the wave outside the well radius (or its extrapolation inside) is the scattering length.
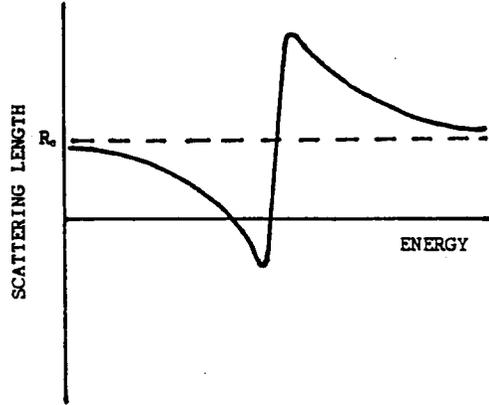

Figure 3. Scattering length as function of energy. At non-zero energy the swing is curtailed.
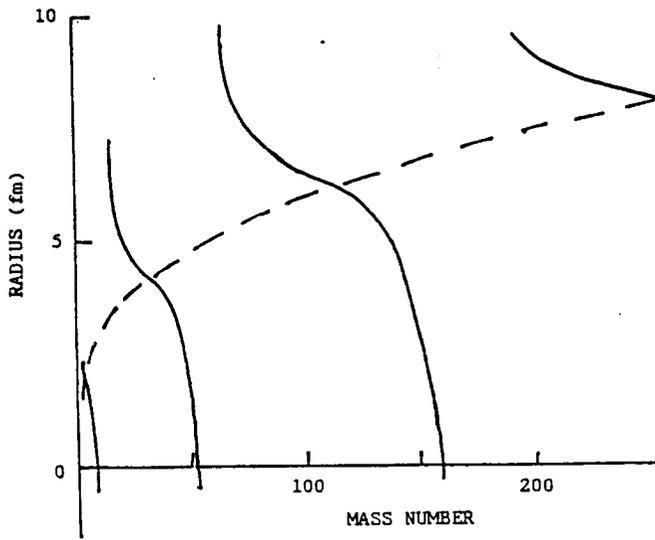

Figure 4.Scattering length as function of mass number.

Real nuclei are much more complex in their reactions with particles than can be represented by a simple potential well. The complexity is illustrated in Fig.5, which shows the energy levels of the compound nucleus formed by adding a neutron to a target nucleus. The binding energy of a neutron in the compound nucleus is several MeV. At this excitation energy, reached by adding a very slow neutron to the target, the level spacing is several tens of keV for very light nuclides, a few keV for medium mass nuclides, and a few eV or less for very heavy nuclides. It is these levels close to zero neutron energy, the resonances and the weakly bound states, that have a major influence on the scattering length. The reason why there is still an apparent potential well effect in the overall pattern of scattering lengths is that the compound nucleus levels retain some 'memory' of the potential resonances, which then exerts a long range influence on the zero energy properties of the scattering.
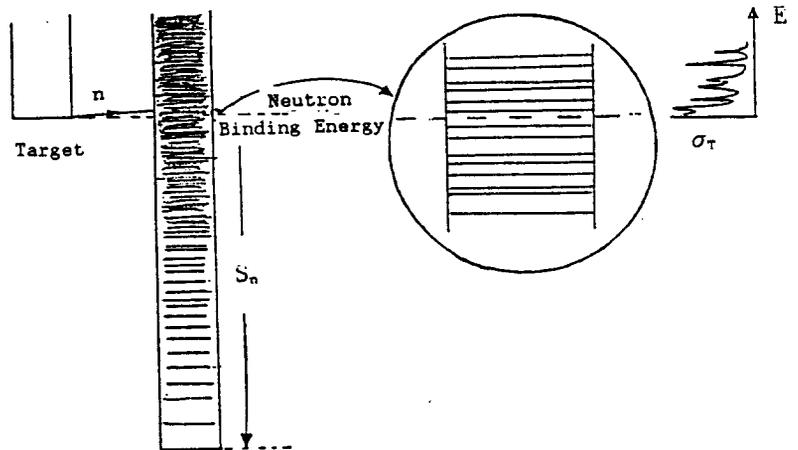
.Figure 5. Nuclear energy levels of compound system. Inset shows enlargement near neutron binding energy with resulting cross-section.

For s-wave neutron interaction, the detailed form of the scattered wave is

$$\Psi^{scat} = \frac{i\sqrt{\pi}}{kr\sqrt{v}} \sum_{s=|j-1/2|}^{j+1/2} [1 - U_s] \exp(ikr)\zeta_s Y_{00}(\vartheta,\varphi) \qquad (5)$$

Here I have introduced the concept of the channel spin s, the total spin formed from the neutron spin $\sigma(=\frac{1}{2})$ and the spin of the target nucleus j; the normalised channel spin wave-function thus formed is denoted by ζ_s. When this is compared with the usual form for the elastic scattering wave-function

$$\Psi^{scat} = \sum_{s=|j-1/2|}^{j+1/2} f_s \exp(ikr)\zeta_s /r \qquad (6)$$

the relation

$$f_s = i(1 - U_s)/2k \qquad (7)$$

is obtained.

The usefulness of this expression lies in the fact that a full formal understanding of the collision matrix element can be obtained from the R-matrix nuclear reaction theory of Wigner and Eisenbud[8] (see also Lane and Thomas[9]). For thermal neutron reactions with nearly all nuclides except the actinides, elastic scattering is accompanied by radiative capture and alpha-emission channels with partial widths that are very small compared with the resonance spacing. For such

reactions an excellent approximation that can be derived from the full theory is the reduced R-matrix formulation. In this, the collision function for elastic scattering can be expressed as

$$U = e^{-2ika}[1 - ika\mathcal{R}]^{-1}[1 + ika\mathcal{R}] \tag{8}$$

where the quantity a is a channel radius (which is usually chosen to equal either the potential well radius of the nucleus or the potential scattering length R'). The reduced R-function for this one-channel case is

$$\mathcal{R} = \Sigma_\lambda \frac{\gamma_{\lambda(n)}^2}{E_\lambda - E - i\Gamma_{\lambda(a)}/2} \tag{9}$$

Here, the E_λ are the formal nuclear energy levels of the (compound) system, with reduced neutron width amplitude $\gamma_{\lambda(n)}$ and absorption width $\Gamma_{\lambda(a)}$ which is the sum of partial widths of all reaction widths of the compound nucleus level λ. The functions U and $\mathcal{R}$ are implicitly labelled by the channel spin s, as are the nuclear levels λ.

If the nucleus can be represented by a simple potential well, the levels λ are just those causing the fluctuations R' apparent in Fig.3 (or 2). If there are no compound nucleus levels (resonances) with E_λ close to E, the effect of these potential well levels can be incorporated into the effective channel radius a, which then equals the potential scattering length R'. The quantity $ka\mathcal{R}$ is then negligible, and since $ka \ll 1$ for low neutron energy, the scattering amplitude f is approximately equal to $-a$, which is the common usage for most neutron scattering work. If compound nucleus levels are significant but distant, so that $\mathcal{R}$ is effectively real and hardly changes over the energy range of interest, the relation is $f \approx -a(1-\mathcal{R})$.

These relations are for a single channel spin. In general a and $\mathcal{R}$ will vary for different isotopes and channel spins. For the general case of a multi-isotope element with non-zero-spin isotopes, the coherent scattering length (for free nuclei) has the well-known form

$$a_{coh.el} = -\Sigma_i w_i \Sigma_s g_{i,s} f_{i,s} \tag{10}$$

where w_i is the fractional abundance of the isotope i in the element and $g_{i,s}$ is the spin-weight factor $(2s + 1)/[2(2j_i + 1)]$ for channel spin s. The total scattering cross-section is

$$\sigma_{sc} = (\pi/k^2)\Sigma_{i,s} w_i g_{i,s} |1 - U_{i,s}|^2 \tag{11}$$

the absorption cross-section is

$$\sigma_a = (\pi/k^2)\Sigma_{i,s} w_i g_{i,s} (1 - |U_{i,s}|^2) \tag{12}$$

and the total cross-section is

$$\sigma_T = 2(\pi/k^2)\Sigma_{i,s} w_i g_{i,s} (1 - \mathrm{Re}U_{i,s}) \tag{13}$$

For many of the heavy nuclides, a single resonance level dominates the energy variation of the collision function for given channel spin. I give here

the single level approximation for the scattering amplitude, with an important extension to include the milder energy dependent effects from more distant resonance terms. This is obtained from eqs.7,8,9. The expression for the scattering amplitude $f_{i,s}$, to second order in a,

$$f = -[a(1-R_{ex})] + 2ka^2 S_{ex}(1-R_{ex}) + \frac{a\gamma_{\lambda(n)}^2[(E_\lambda+\Delta_\lambda-E) + ka\Gamma_\lambda(1-R_{ex})]}{(E_\lambda+\Delta_\lambda-E)^2 + \Gamma_\lambda^2/4}$$

$$+i\left\{[aS_{ex} + ka^2(1-R_{ex})^2 - ka^2 S_{ex}^2] + \frac{a\gamma_{\lambda(n)}^2[\Gamma_\lambda/2 + 2ka(E_\lambda+\Delta_\lambda-E)(1-R_{ex})]}{(E_\lambda+\Delta_\lambda-E)^2 + \Gamma_\lambda^2/4}\right\} \quad (14)$$

the labels i,s being implicit. Here, the quantities R_{ex}, S_{ex} are measures of the real and imaginary contributions of other levels; when these are some distance from the level λ the distant level quantities can be described as simple polynomials:

$$R_{ex} = A_r + B_r(E - E_0) + C_r(E - E_0)^2 + \ldots \quad (15)$$

$$S_{ex} = A_i + B_i(E - E_0) + C_i(E - E_0)^2 + \ldots \quad (16)$$

where E_0 is some approximately central point in the energy range of interest. The width Γ_λ is the total resonance width of the most significant resonance λ; it is the sum of a neutron width $\Gamma_{\lambda(n)}$ ($= 2ka\gamma_{\lambda(n)}^2$, to second order in ka and distant level quantities) and the absorption width $\Gamma_{\lambda(a)}$. The quantity Δ_λ is a level shift that can usually be neglected at the very low neutron energies considered in this paper.

The generalised single level formula of eq.14 can be used to analyze cross-section and scattering length data by least square fitting to obtain an assessment of the coherent scattering length data from neutron energy close to zero up to approximately 0.5 eV. An alternative way of treating the potential well effects of Figs.1-3 is to incorporate their long-range effects empirically in the constant A_r of eq.11, and to use the convential nuclear potential radius as the channel radius a:

$$a = 1.16A^{1/3} + 0.6 \text{ fm.} \quad (17)$$

The pivot energy E_0 is also chosen in advance. With these constraints the parameters E_λ, $\gamma_{\lambda(n)}^2$, $\Gamma_{\lambda(a)}$, A_r, B_r, ..., A_i, B_i, ... for each isotope and channel spin are then determined from the data. The free atom nuclear coherent scattering lengths can then be determined from eqs.10 and 6. Because there is generally very much more detailed cross-section data available on a given nuclide than data on scattering lengths, it is possible to learn a great deal about the latter by this procedure.

3. Examples of deduced scattering lengths

The main example that I shall use to demonstrate the possibility of extraction of the energy dependent, complex scattering length from cross-section data is the case of samarium and its isotopes, also discussed in the introduction and Table 1.

8

The total cross-section of natural samarium[10] is shown in Fig.6. The strong resonance at approximately 0.1 eV is known (from measurements on separated isotopes) to belong to the target ^{149}Sm (present at 13.9% in the natural element), and the spin s of this resonance has been ascertained by polarised neutron and target techniques[11] to be $s = 4$ (the target spin $j = 7/2$). The resonance parameters have been rather well determined[12]. The scattering cross-section as a function of energy across the resonance has been measured[13]. The refitting of all these data gives a set of resonance parameters rather close to those found in the literature together with parameters for the slowly varying contribution of the other levels. From these, the coherent scattering length behaviour of ^{149}Sm is calculated; it is shown as the broken curve in Fig.7.

The data points shown in Fig.7 have not been used in the fitting. They are measurements of the real part of the neutron scattering length of ^{149}Sm, made by interferometry techniques[6], and are not generally found in compilations. It is clear that the broken curve represents the data rather well but not optimally so. A refit of the collision function parameters to include these data leads to the calculated full curve, which is obviously better, but not drastically so. It is clear that it is possible to calculate the energy dependence of coherent scattering lengths quite reliably from cross-section data of this quality.

If we now use the deduced parameters of the collision function of ^{149}Sm with the measured long wave-length coherent scattering lengths of ^{152,154}Sm and the natural element we can determine the energy dependent scattering length of natural Sm and the abundance-weighted average of all the
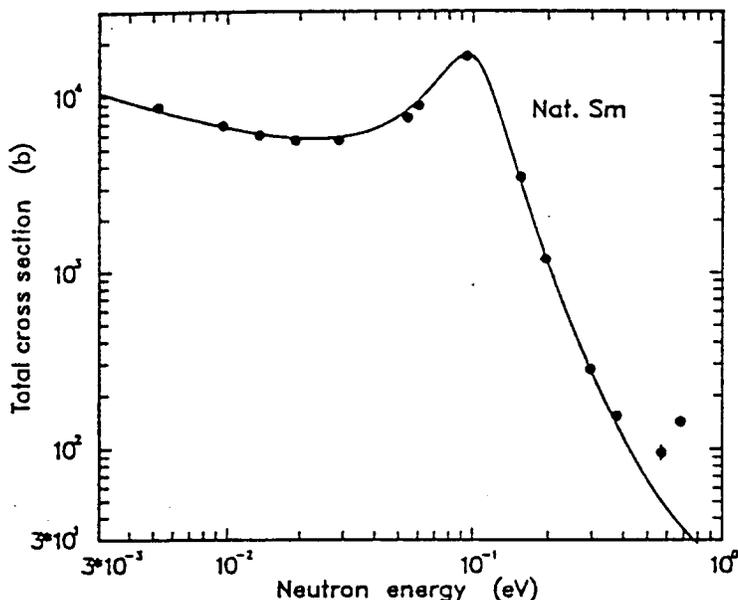

Figure 6. The neutron total cross-section of natural samarium.
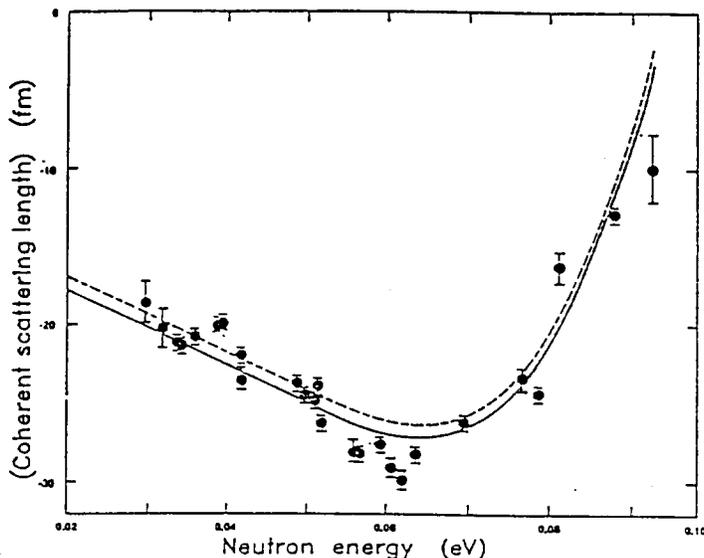
Figure 7. Real part of the coherent scattering length of ^{149}Sm. Curves and data are explained in the text.

9

isotopes except 149, 152, and 154. The coherent scattering length of the natural element is shown as the full curve of Fig.8. This can be compared with some energy dependent measurements[2] which have not been used in the fitting procedure. It is clear that the agreement is very good, again giving us confidence in our procedure.

The analysis does not give us confidence in the overall set of numbers in Table 1, however. The weighted average of the scattering lengths of the isotopes for which measurements do not seem to be available is determined in our fitting as 8.5 fm. The value computed from the entries of Table 1 is 19 fm. The discrepancy is wide, and a large part of it comes from the extraordinarily high value given in ref.5 for ^{148}Sm. If this were really so large, it would have to be due to a very strong bound level in the ^{148}Sm + n system, and no evidence in the form of a very high total scattering or capture cross-section is available to support this hypothesis.

Phil Seeger and I have carried out analysis of this kind on the available cross-section data of all the elements of the rare earth series that have obvious resonance effects[14]. In general we have taken our analysis and computation of coherent scattering lengths up to 0.5 eV (wavelength 0.41 Å). The calculated, and recommended, energy dependence for all the isotopes and some natural elements that display resonance behaviour is shown in Fig.9. We plan to make a similar systematic study of other nuclides at a later date.

4. Some effects of resonance behaviour in scattering lengths.

4.1. Small angle scattering and total reflection

The striking features of the coherent scattering lengths in the examples shown in Fig.9 are of course the large imaginary component and the very large real component above the resonance energy. The former gives rise to strong absorption; this severely limits the penetration depth of neutrons, but also gives a phase variation that can yield additional information from scattering measurements.

^{115}In has a strong resonance at 1.46 eV. From the resonance parameters the scattering length can be calculated. Its energy behaviour above 1 eV is shown in Fig.10. Experiments have been carried out to detect the anomalous total scattering caused by this[15]. The calculated scattering from a plane surface of indium at various neutron energies is shown in Fig.11. There is a striking variation in the angle of quasi-critical-scattering with a maximum reached at about 1.6 eV, and this is greater than at any energy above 0.1 eV

Resonance critical scattering is probably observable at energies well above 1 eV for several materials. An example is shown for ^{152}Sm, which has a particularly strong resonance at 8 eV, in Fig.12.

An interesting example of the possible application of resonance scattering is being explored by Hjelm, Seeger and Thiagaryan[16]. They have suggested the use of the strong contrast provided by the large change in coherent scattering length over a small range of neutron energy (e.g. 63 fm from 0.07 eV to 0.11 eV in ^{149}Sm) to locate the position of the metallic atom in large metallo-organic molecules, using small angle scattering diffractometers on white neutron pulsed sources.

4.2. Bragg reflection

Despite the strong absorption, strong Bragg reflections can be obtained at neutron energies close to resonance. One of the strongest resonances known at low energies is found in the cross-section of ^{240}Pu at 1.04 eV. A calculated Bragg reflection from a single crystal of PuO$_2$ is shown in Fig.13. This is the [12,4,0] reflection at the energy 1.04 eV. It is calculated for a crystal thickness of 2.10^4 atomic layers, by using the Darwin multiple scattering formalism originally developed for X-ray diffraction. The angle-integrated line strength over the energy range 0.9 eV to 1.2 eV is shown in Fig.14. For this thickness of crystal the reflection strength

Figure 8. Real part of the coherent scattering length of natural samarium. Curves and data are explained in the text.

qualitatively follows the resonance scattering cross-section. For increasing crystal thickness the wings rise, the centre remaining almost constant owing to primary extinction and absorption, until for very great thickness there is little evidence of the resonance.

These general features suggest that resonance scattering could be used to explore the structure of surface layers of intermediate thickness, although not as low as a few mono-layers. It should also be remembered that, for nuclides with odd numbers of protons, neutrons or both the resonance scattering is sensitive to the relative spin polarisation of the neutron beam and the target nucleus, and could therefore be useful in studies of magnetic materials at low temperatures.

4.3. Powder diffraction

Because of the strong absorption resonance scattering would not appear at first sight to be a useful effect in powder diffraction studies. Nevertheless, in refinement analyses of the Reitveld kind it is obviously important to include as well as possible the wave-length variation of the scattering length, and the changing ratio of the imaginary to real components offers the opportunity to gain some phase information.

Even relatively weak resonances complicate the analysis of a powder pattern. An example, due to Goldstone and Lawson[17], is shown in Fig.15; this is NpD$_{2.67}$, which, at room temperature has a face-centred cubic cell, with the deuterium atoms occupying tetrahedral and octohedral sites in different proportions. The absorption dips in the overall scattering (coherent and incoherent) due to the resonances at 0.49 eV and 1.32 eV are very strong. Greater detail for the resonance region is shown in Fig.16. In this some evidence of diffraction lines is to be found in the resonance minimum. Indeed, these, as well as the lines above the resonance (in energy), may be surprisingly strong relative to the lines at longer wavelengths below the resonance.

A preliminary analysis indicates that the relative magnitude of these groups of lines certainly cannot be explained on the assumption of a constant
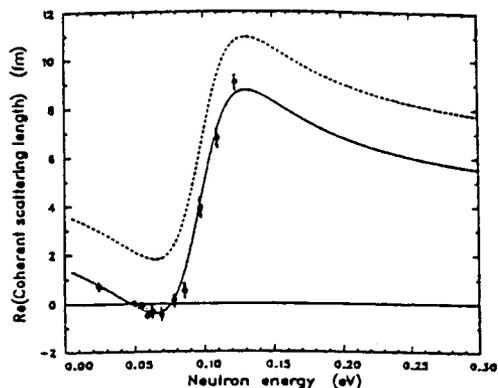
11
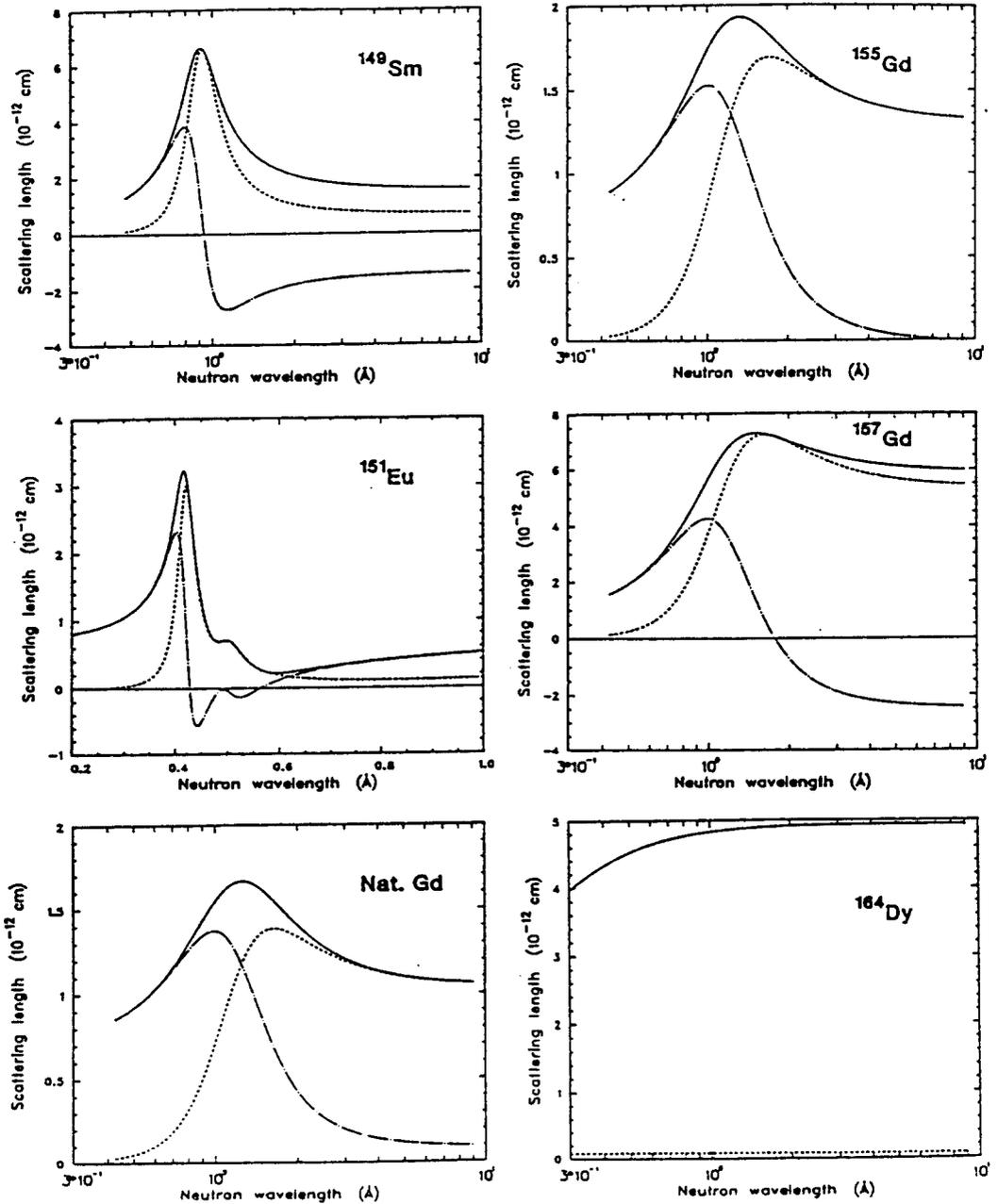
Figure 9. The coherent scattering lengths of the rare earth nuclides with resonance effects in the thermal and epithermal neutron energy region. The dash-dot curve is real, dot is imaginary, and full is the modulus.
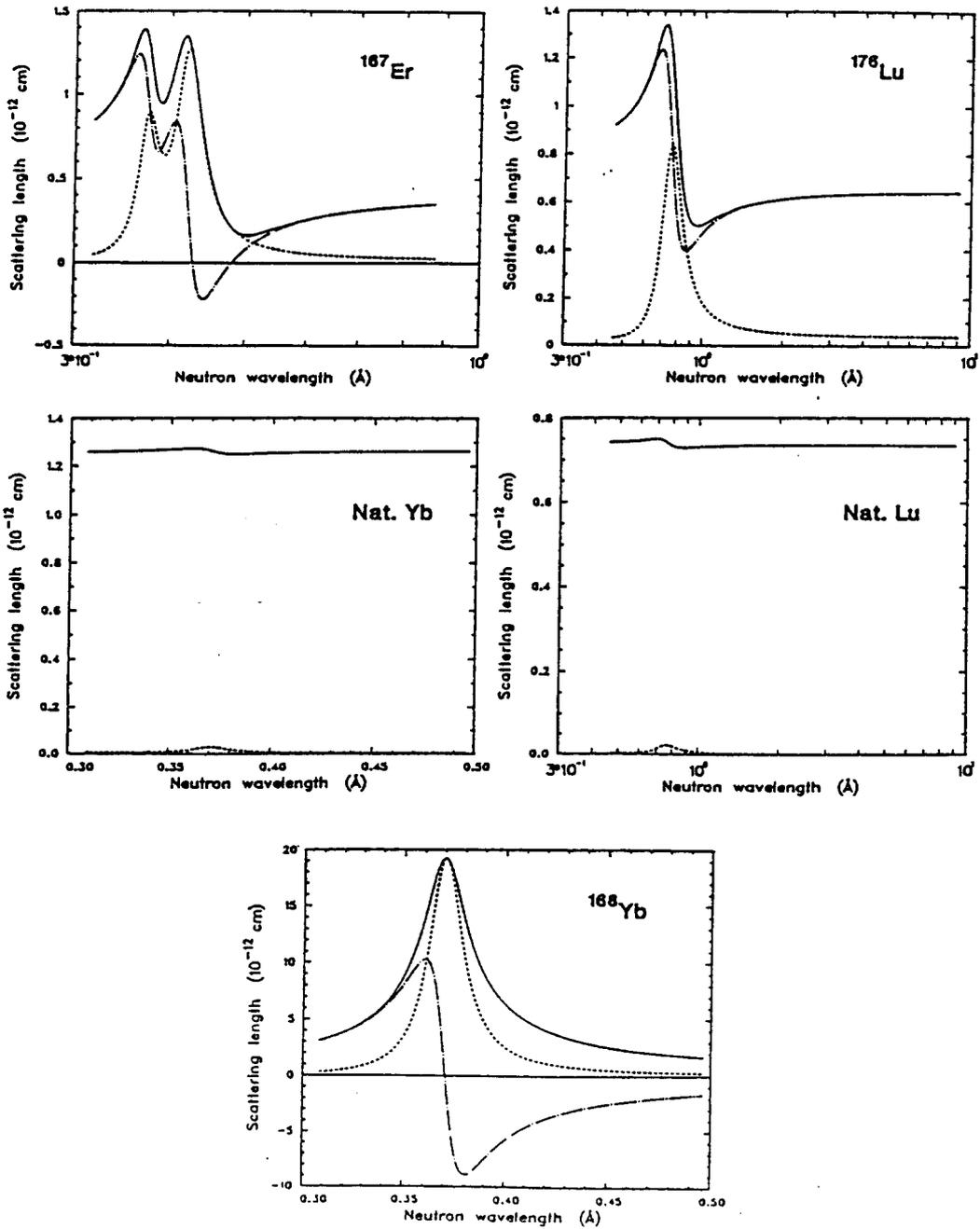
Figure 9. Continued
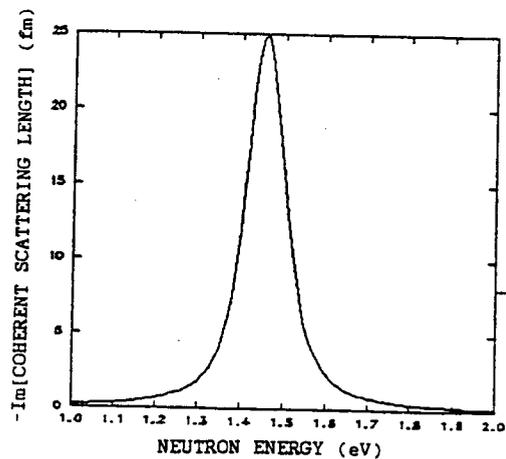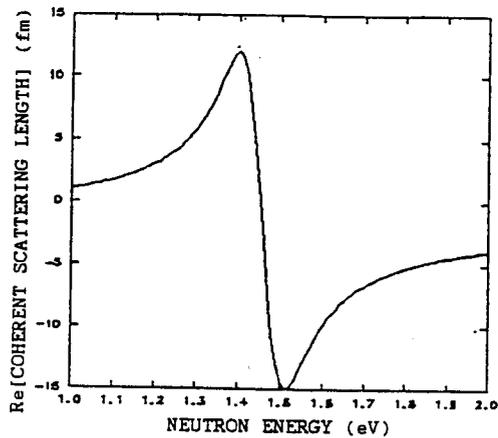
Figure 10. Real and imaginary scattering length of indium as function of neutron energy.
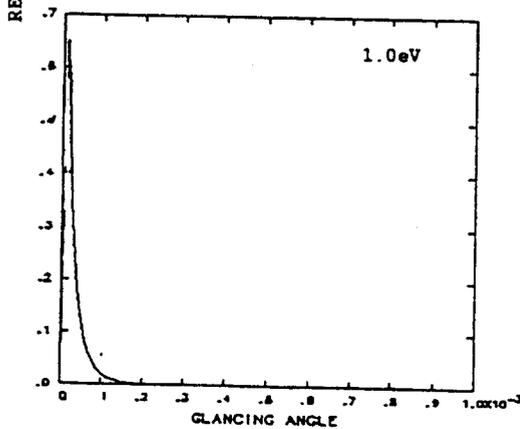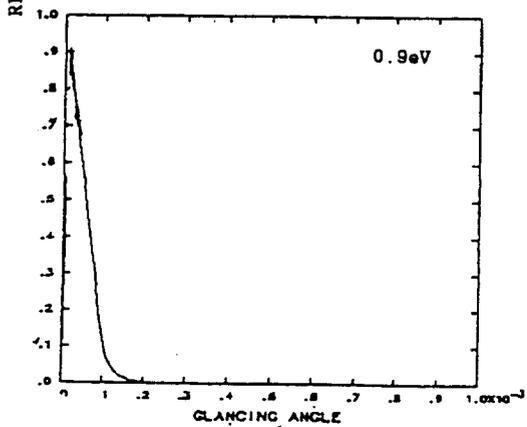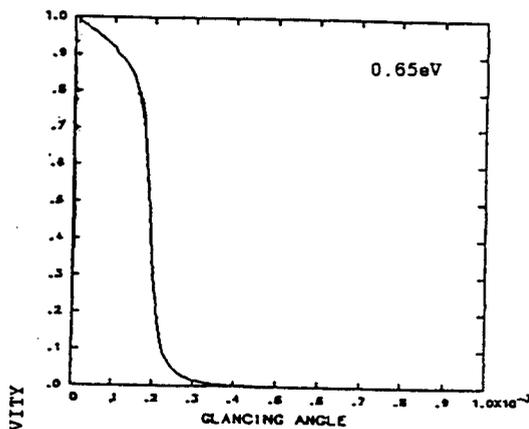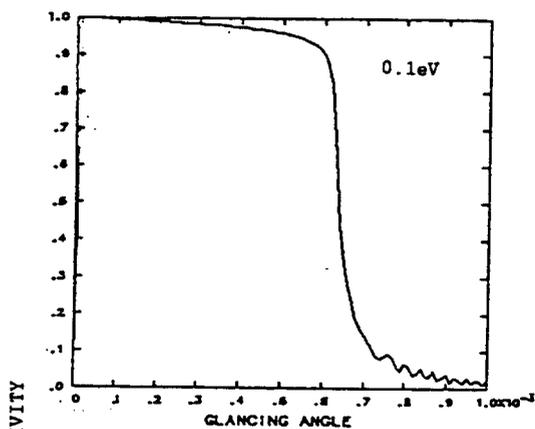
Figure 11. Reflectivity of indium as function of glancing angle for a range of neutron energies.
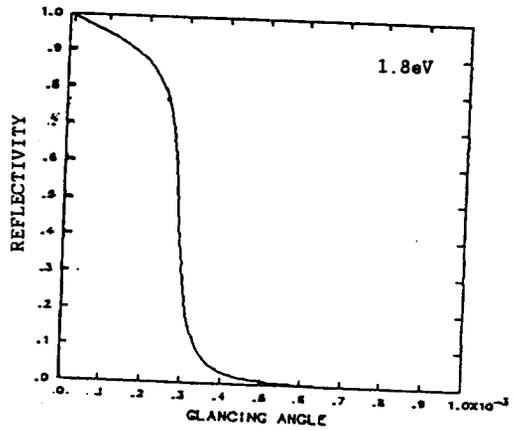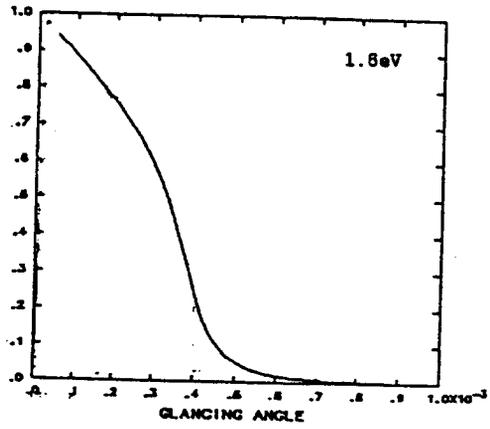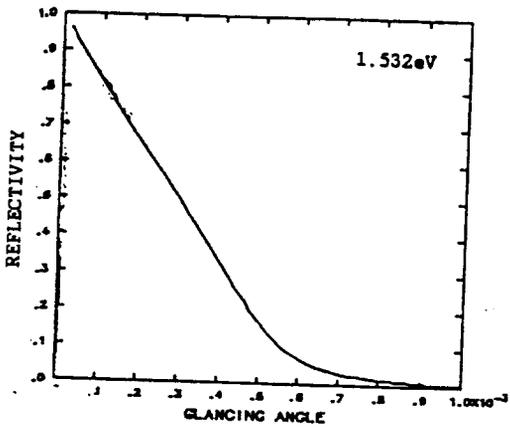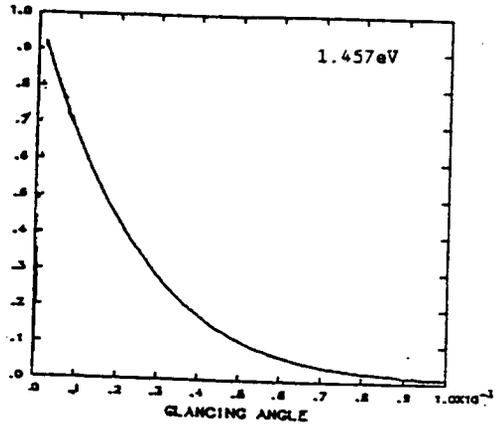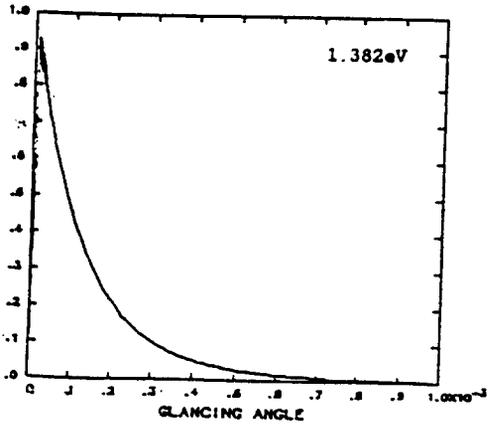
Figure 11. Continued
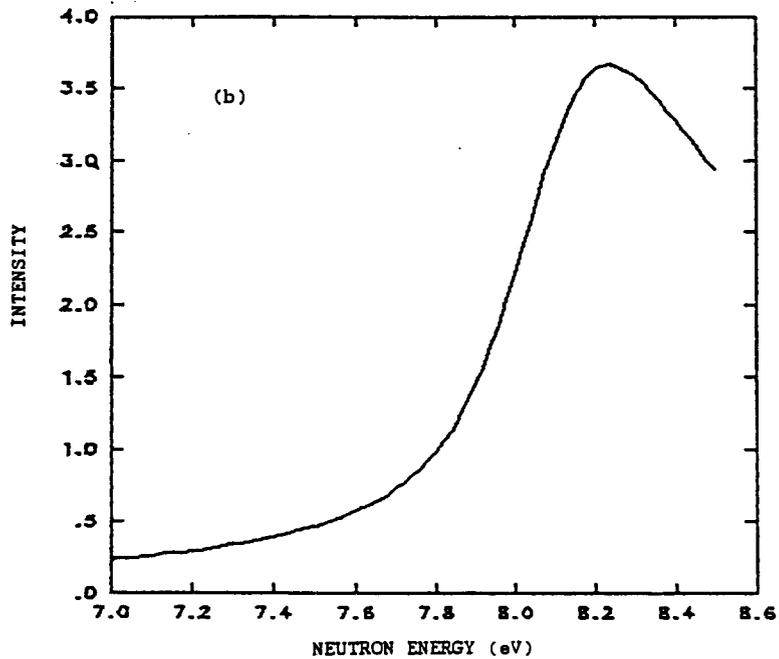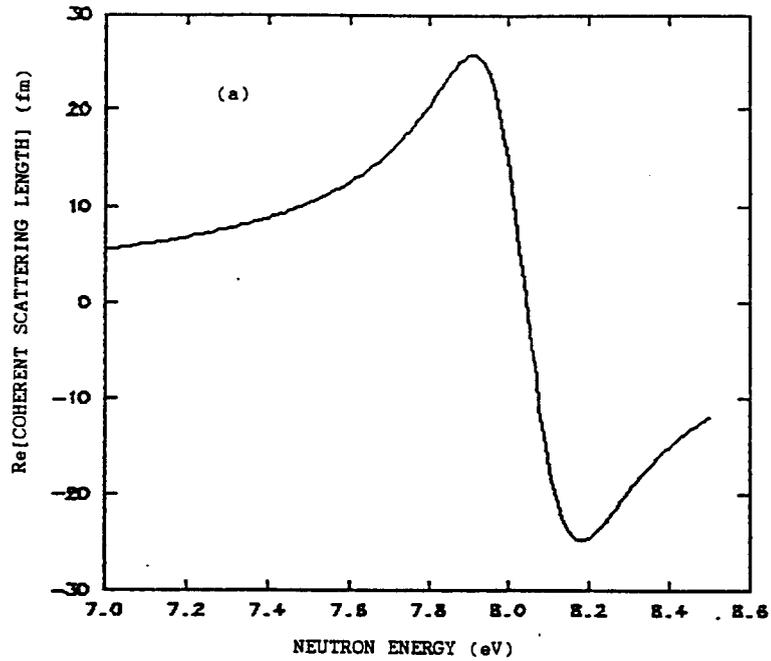
Figure 12. Critical reflection properties near the 8 eV
resonance of ¹⁵²Sm. Part (a) shows the real part of the
scattering length. Part (b) shows the neutron reflection
strength integrated from 0 to 0.1 mrad as function of
neutron energy.
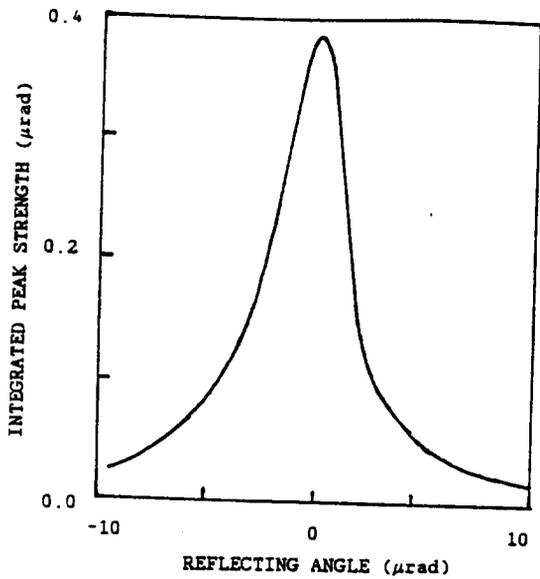
Figure 13. Detailed angular dependence of Bragg reflection line for ^{240}PuO$_2$ for neutrons of 1.068 eV.
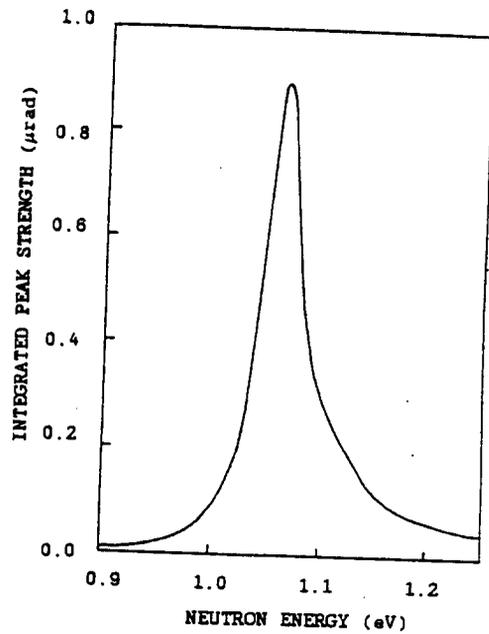
Figure 14. Energy dependence of Bragg reflection strength for reflection from 10^6 atomic layers as function of neutron energy near the 1.04 eV resonance of ^{240}Pu.
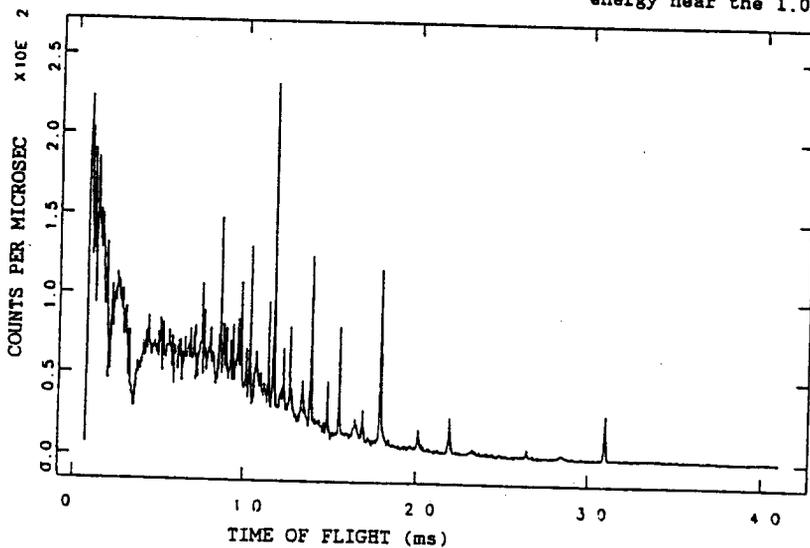
Figure 15. Powder diffraction pattern from NpD$_{2.8}$, as function of neutron time-of-flight.

Figure 16. Powder diffraction pattern from NpD$_{2.8}$, as function of neutron time-of-flight, showing resonance region in greater detail
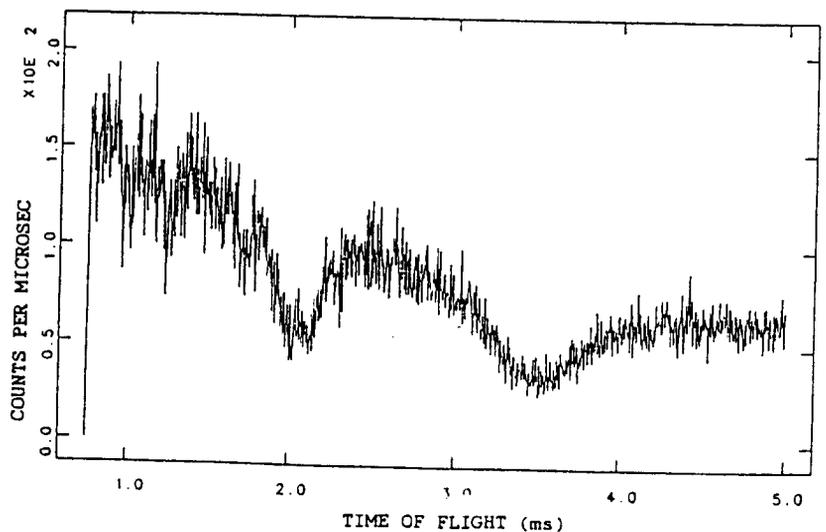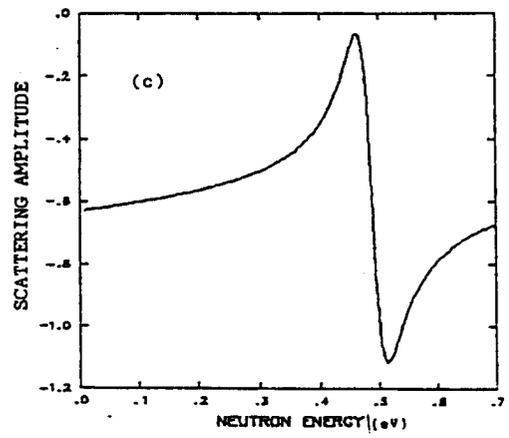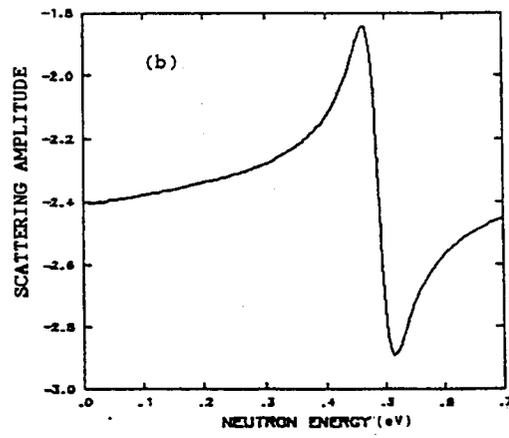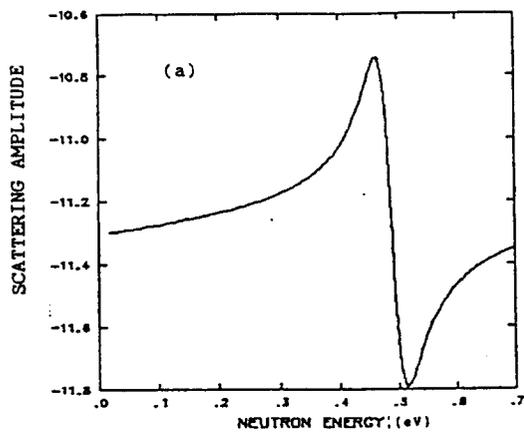
17

Figure 18. Diffraction line strengths for NpD$_{2.6}$, calculated as function of neutron energy in the neutron energy. Line classes as in Fig.17.

Figure 18. Diffraction line strengths for NpD$_{2.6}$, calculated as function of neutron energy in the neutron energy. Line classes as in Fig.17.

18
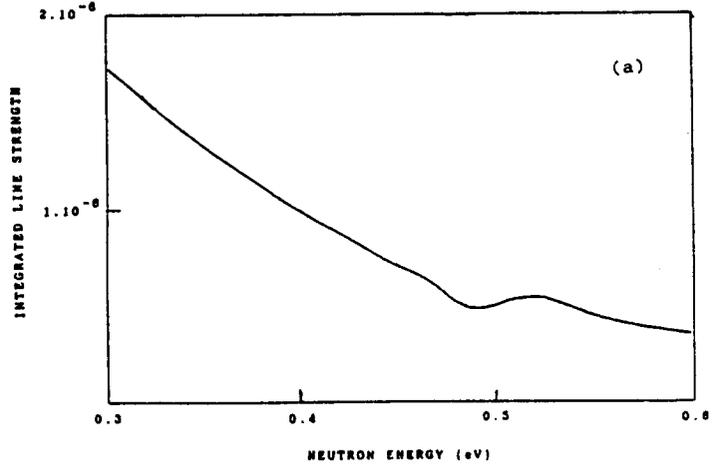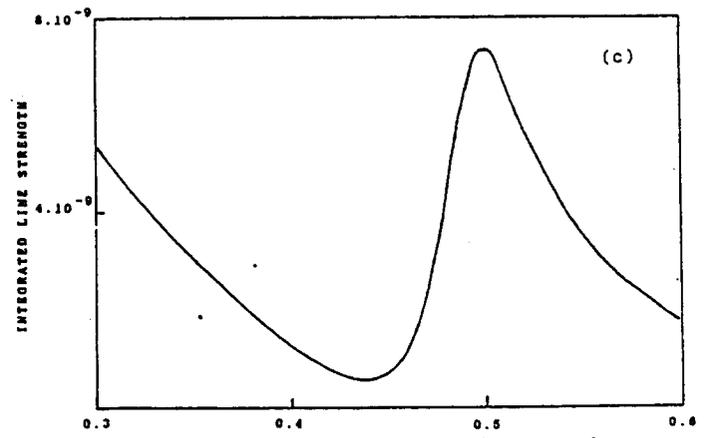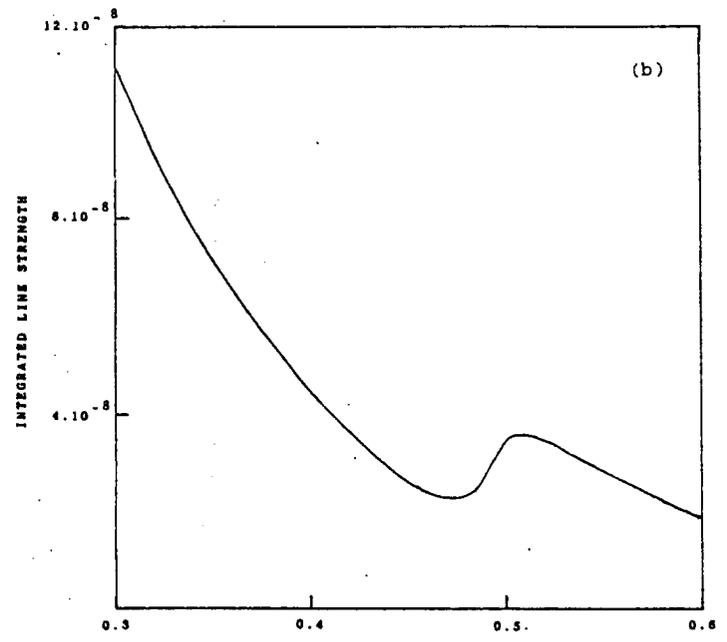
coherent scattering length for neptunium, or even with the inclusion of the resonance variation if the phonon frequency for the deuterium is assumed to be the same as that for Np. The calculated scattering amplitude for the latter assumption is shown for the three different classes of the order of reflection in Fig.17. The largest amplitude, in general, is for reflection order satisfying the relation $h + k + l = 4n$ where n is an integer, and the next largest is that for $h + k + l = 2n + 1$. The corresponding energy dependence of the angle-integrated line strength is shown in Fig.18. It is clear that the contribution of deuterium is too high too allow the resonance effect for the $h + k + l = 4n$ reflections to be very significant. Inelastic scattering measurements[18] have revealed, however, that very high frequency phonons reside on the deuterium, which will give it a small Debye-Waller factor, especially at the high energies corresponding to the resonance region.

References

1. Rauch H and Tuppinger D (1983) *Zeit.Phys.***A322**, 427
2. Engle D W and Koetzle T F (1984) *Act.Cryst.* **A40**, 99
3. Sikka (1969) *Act.Cryst.* **A25**, 621
4. Mughabghab S F (1984) *Neutron Cross Sections* Vol.1 Pt.B (Academic, Orlando)
5. Sears (1986) in *Methods of Experimental Physics* **23A**, 521
6. Word R E and Werner S A (1982) *Phys.Rev.* **B26**, 4190
7. Koehler W C and Wollan E O (1953) *Phys.Rev.* **91**, 597
8. Wigner E P and Eisenbud L (1947) *Phys.Rev.***72**,129
9. Lane A M and Thomas R G (1958) *Rev.Mod.Phys.***30**,257
10. Sailor V L, Landon H H and Foote H L (1954) *Phys.Rev.***96**,1014
11. Marshak H, Postma H, Sailor V L, Shore F J and Reynolds C A (1962) *Phys.Rev.***128**,1287
12. Marshak H and Sailor V (1958) *Phys.Rev.***109**,1219
13. Brockhouse B N (1953) *Can.J.Phys.* **31**, 432
14. Lynn J E and Seeger P A 1989 acc. for publ.in *At.Data & Nuc.Data Tables*
15. Hjelm R, Seeger P A and Thiyagarjan P, private communication
16. Batigun C M and Brugger R M (1988) *J.App.Cryst.* **21**, 54
17. Goldstone J A, Lawson A C, Cort B and Ward J W 1988 unpublished
18. Goldstone J A, Vorderwisch P, Cort B, Lawson A C and Ward J W 1988 to be published